

# EDGE2D modelling of JET and ITER including the combined effect of guiding centre drifts and an edge transport barrier

S.K. Erents<sup>a,\*</sup>, W. Fundamenski<sup>a,1</sup>, G. Corrigan<sup>a</sup>, G.F. Matthews<sup>a</sup>,  
R. Zagorski<sup>a,b</sup>, EFDA-JET Contributors<sup>2</sup>

<sup>a</sup> Euratom/UKAEA Fusion Association, Culham Science Centre, Abingdon, Oxon OX14 3DB, UK

<sup>b</sup> Institute of Plasma Physics and Laser Microfusion, Warsaw, Poland

## Abstract

Code predictions of parameters in the pedestal region of high power H-mode discharges on JET have been performed using the EDGE2D code including (i) self-physically and chemically sputtered carbon impurities, (ii) guiding centre drifts with realistic core boundary conditions, and (iii) an imposed edge transport barrier (ETB). For a transport barrier with a minimum  $D_{\perp}^{\min} < 0.5 \text{ m}^2 \text{ s}^{-1}$  the pedestal (core) carbon content is increased along with the associated radiation by up to 65%, compared with the no drift case. The result is a reduction in pedestal electron temperature and an increase in pedestal density by  $\sim 30\%$ , (such that pressure is unaffected), and inner target detachment. Without drifts, the pedestal pressure, stored energy and energy confinement time increase as  $(D_{\perp}^{\min})^{-1/2}$ , which is not modified by the inclusion of drifts. Reasonably good agreement with experimental measurements on JET is achieved for a moderate ETB strength of  $D_{\perp} = 0.4 \text{ m}^2 \text{ s}^{-1}$ . Preliminary results for ITER are discussed.

© 2007 Elsevier B.V. All rights reserved.

PACS: 52.40.Hf; 52.55.Fa; 52.30.-q

Keywords: EDGE modelling; EDGE2D; JET; ITER; Pedestal

## 1. Introduction

Recent modelling of the JET edge plasma using the EDGE2D fluid code has shown that inclusion

of guiding centre (GC) drifts can improve the agreement with experimental data, e.g. with the level of divertor power asymmetry [1,2]. However, in these studies, drifts were activated only in the SOL region and hence their impact on edge (pedestal) plasma profiles was not investigated. In the present study, drifts are activated everywhere in the EDGE2D computational domain by introducing an improved core boundary condition on the innermost computational ring. In addition, an edge transport barrier (ETB) is imposed by reducing the prescribed radial

\* Corresponding author.

E-mail addresses: [ske@jet.uk](mailto:ske@jet.uk) (S.K. Erents), [wfund@jet.uk](mailto:wfund@jet.uk) (W. Fundamenski).

<sup>1</sup> Presenting author.

<sup>2</sup> See the Appendix of J. Pamela et al., Fusion Energy 2004 (Proc. 20th Int. Conf. Vilamoura, 2004) IAEA, Vienna (2004).

diffusivities of particles and heat in the edge region, using a realistically chosen pedestal width and diffusivity profile. Physical and chemical sputtering of carbon, which leads to variable radiation levels in core and SOL, are also included. Previously, EDGE2D reproduced ELMy H-mode plasmas using an ETB and imposed radial pinch terms [3]. The new results represent the first successful reconstruction of both target and pedestal profiles with an ETB and self-consistent drifts, without an imposed radial pinch.

## 2. Improvements to the EDGE2D drift model

The previous EDGE2D drift model was consistent with that implemented in the TECXY [4] and B2-SOLPS5 codes [5]. Although, the magnetisation drift term used in EDGE2D was more complicated, the final equation set was the same; to simplify future development and code-code benchmarking, the description used in [4] has now been implemented. The main drawback of the previous EDGE2D drift model is the fact that the radial electric field on closed magnetic surfaces (pedestal plasma) was not calculated self-consistently. This shortcoming is now circumvented by introducing a new boundary condition which imposes a constant plasma density and temperature on the core boundary (innermost core ring), for any given input particle and energy fluxes. The magnetisation drift term, which previously gave rise to a large, unphysical radial drift flux on the core boundary, is now cancelled analytically by the gradient-B drift term, such that in the absence of poloidal gradients, the radial drift velocity vanishes exactly. Note that since both magnetisation and gradient-B terms are large, they give rise to an equally large Pfirsch-Schluter flux.

## 3. JET Model predictions

To simulate H-mode discharges on JET, an edge transport barrier (ETB) is included in EDGE2D by reducing the radial perpendicular transport. This barrier is formed by a particle transport coefficient  $D_{\perp}$  falling rapidly from  $1.0 \text{ m}^2 \text{ s}^{-1}$  at 50 mm inside the separatrix to a value  $D_{\perp}^{\text{min}}$ , then rising rapidly again at the separatrix to a value of  $1.0 \text{ m}^2 \text{ s}^{-1}$  again at 10 mm outside the separatrix. These values are at the outer mid-plane, and assumes poloidal flux expansion.  $D_{\perp}^{\text{min}}$  is varied, however a minimum  $D_{\perp}^{\text{min}} = 0.1 \text{ m}^2 \text{ s}^{-1}$  is chosen on the basis of previous publications [6,7]. A heat transport coefficient,

$\chi_{\perp} = 2.5 D_{\perp}$  is assumed, again from [6,7] and simple transport theory. The shape of the barrier close to the separatrix matches experimental measurements and Onion-Skin modelling as reported in [7]. Boundary conditions are set such that the perpendicular ion velocity is  $\sim 0$  at the top of the pedestal,

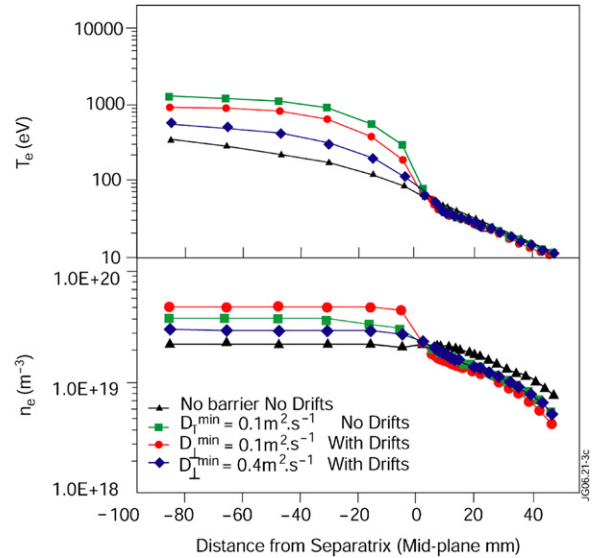


Fig. 1. Electron temperature and density profiles at outer mid-plane for various boundary conditions of transport and drifts. Separatrix density =  $2.3 \times 10^{19} \text{ m}^{-3}$ ,  $P_{\text{in}} = 12 \text{ MW}$ .

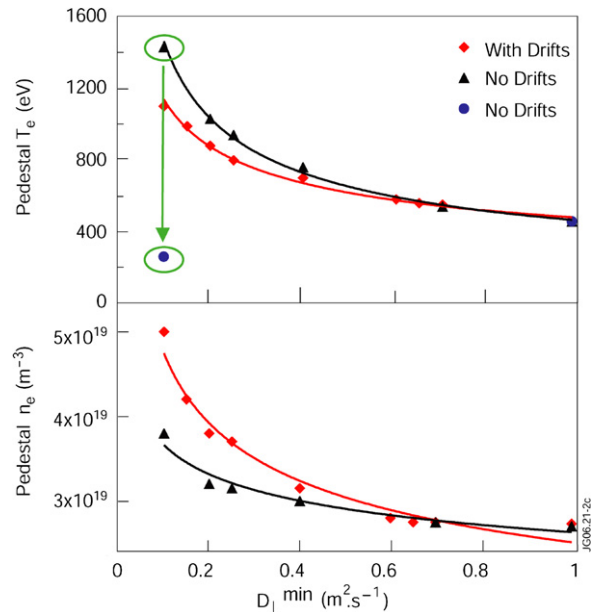


Fig. 2. Effect of transport barrier height on  $T_{\text{ped}}$  and  $n_{\text{ped}}$  at the top of the transport barrier, (innermost core ring). The lower  $T_{\text{ped}}$  point at  $D_{\perp}^{\text{min}} = 0.1 \text{ m}^2 \text{ s}^{-1}$  shows a temperature collapse, also predicted by the code. Separatrix density =  $2.3 \times 10^{19} \text{ m}^{-3}$ .

as expected for low collisionality in this region, which results in poloidally uniform and very low ( $<20 \text{ m s}^{-1}$ ) total perpendicular velocities throughout the pedestal region. A variable minimum,  $0.1 \text{ m}^2 \text{ s}^{-1} < D_{\perp}^{\text{min}} < 1 \text{ m}^2 \text{ s}^{-1}$  has been used in separate code runs to determine the effect of barrier height on pedestal temperatures and densities at the top of the pedestal ( $T_e^{\text{ped}}$ ,  $n_e^{\text{ped}}$ , where  $D_{\perp} = 1 \text{ m}^2 \text{ s}^{-1}$ ).

A number of typical Type-I ELMy H-mode JET discharges with strong additional fuelling (2.5 MA/2.4 T,  $\sim 12 \text{ MW}$  NBI,  $n/n_{\text{GW}} \sim 0.7\text{--}0.9$ ), cases have been modelled, with  $P_{\text{in}} = 12 \text{ MW}$ ; a 2:1 partition of power between ions and electrons has been assumed [8]. Mid-plane profiles  $T_e(r)$  and  $n_e(r)$  as predicted from the code are shown in Fig. 1, for various boundary conditions of transport and drifts. In the absence of drifts, an ETB increases  $T_e^{\text{ped}}$  and  $n_e^{\text{ped}}$ , such that the pedestal pressure  $p_e^{\text{ped}}$  increases roughly as  $(D_{\perp}^{\text{min}})^{-1/2}$ . When drifts are included,

$T_e^{\text{ped}}$  is reduced by 30% and  $n_e^{\text{ped}}$  is increased by 30% such that  $p_e^{\text{ped}}$  remains constant.

In Fig. 2, the effect of ETB strength on  $T_e^{\text{ped}}$  and  $n_e^{\text{ped}}$  is shown, each point representing a separate converged solution code. The pedestal pressure,  $p_e^{\text{ped}}$ , the pedestal stored energy,  $W_{\text{ped}}$ , and energy confinement time,  $\tau_E \sim W_{\text{ped}}/P_{\text{SOL}}$ , increase roughly as  $(D_{\perp}^{\text{min}} = \frac{2}{5} \chi_{\perp}^{\text{min}})^{-1/2}$ , and are not affected by the inclusion of drifts. The lower  $T_e^{\text{ped}}$  point at  $D_{\perp}^{\text{min}} = 0.1 \text{ m}^2 \text{ s}^{-1}$  represents radiative collapse and the formation of an X-point MARFE. For  $D_{\perp}^{\text{min}} < 0.5 \text{ m}^2 \text{ s}^{-1}$ , inclusion of drifts increases the radiated power by up to 65%, which is caused by a corresponding increase in carbon impurity content, mostly in the pedestal (core) region, see Table 1, where  $D_{\perp}^{\text{min}} = 0.1 \text{ m}^2 \text{ s}^{-1}$ . The increased carbon radiation, Fig. 3, is partly offset by reduced atomic energy losses (line radiation and charge exchange), but the net effect is to increase the total radiative fraction. The increased cooling of both the pedestal

Table 1  
The computed power and particle balance between core, SOL, wall and divertor targets

Parameter	Species	Without drifts	With drifts	Difference	Ratio
<i>Radiation (MW)</i>					
Core	C	1.0	5.3	4.3	5.3
Outer divertor + Private	C	1.5	0.9	-0.6	0.6
Inner divertor + Private	C	1.3	0.1	-1.2	0.08
Atomic processes	D	4.5	3.0	-1.5	0.7
Total		8.3	9.3	1.0	1.1
<i>Electron power flow (MW)</i>					
Core to SOL (Conductive)	D	4.9	4.4	-0.5	0.9
Core to SOL (Convective)	D	0.5	1.0	0.5	2
Total	D	5.4	5.4	0	1
<i>Carbon content (<math>10^{18} \text{ m}^{-3}</math>)</i>					
Core	C	8	12	4	1.5
SOL	C	3	5.9	2.9	2
Outer divertor	C	1.3	0.7	-0.6	0.5
Inner divertor	C	1.4	4	2.6	2.8
Total	C	13.7	22.6	8.9	1.6
<i>Plas. Pow. to Walls, Targets (MW)</i>					
Total outer target	D	2.0	1.6	-0.4	0.8
Total inner target	D	0.8	<0.1	-0.7	$\sim 0.1$
Total SOL wall	D	0.8	0.6	-0.2	0.75
Total	D	3.6	2.3	-1.3	0.6
<i>Fluxes (<math>10^{21} \text{ s}^{-1}</math>)</i>					
Core to SOL (Conductive)	D	8	16	8	2
Core to SOL (Convective)	D	-	0.2	0.2	-
SOL to divertor	C	0.45	2	1.55	4.4
SOL to wall	C	2	2	0	1

$D_{\perp}^{\text{min}} = 0.1 \text{ m}^2 \text{ s}^{-1}$ .

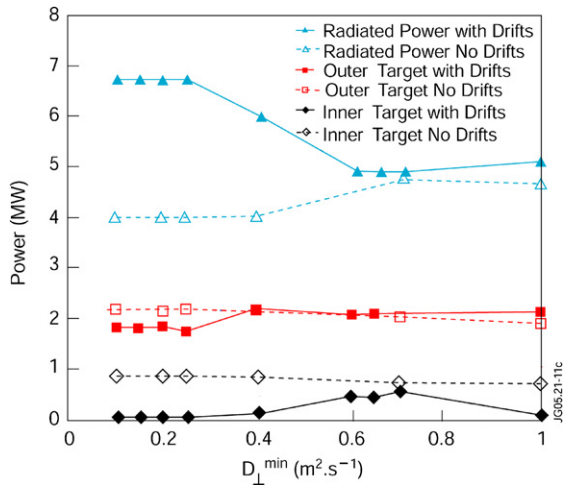


Fig. 3. Total radiated power and power to outer and inner targets with and without drifts.

and divertor plasmas leads to earlier inner target detachment.

#### 4. Comparison with experiment

A number of typical type-I ELMy H-mode discharges with strong additional fuelling (2.5 MA/2.4 T,  $\sim 12$  MW NBI,  $n/n_{GW} \sim 0.7$ – $0.9$ ),  $n_e^{sep} = 1.1 \times 10^{19} \text{ m}^{-3}$  (JET shot 53089) and  $2.3 \times 10^{19} \text{ m}^{-3}$  (JET shot 53090) have been modelled using EDGE2D with both ETB and drifts.  $T_e(r)$  profiles from a variety of edge diagnostics are shown in Fig. 4, together with model predictions. Note that the edge diagnostic data is not reliable in the SOL region. The code simulations are shown as solid and dashed lines in the plot. It was found that an

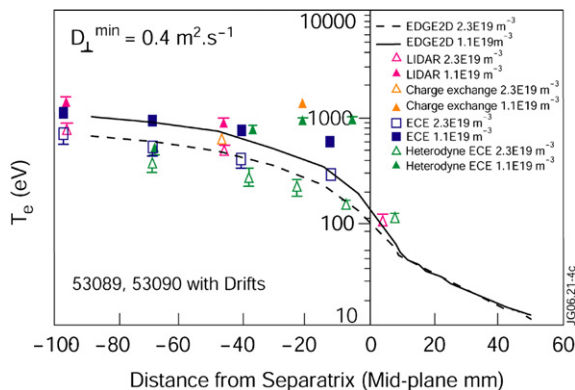


Fig. 4. Electron temperature profiles at outer mid-plane showing two different separatrix densities as input to the code. Measured electron temperature data from various diagnostics at these two densities is also shown.

ETB with  $D_{\perp}^{\min} = 0.4 \text{ m}^2 \text{ s}^{-1}$  gives the best match to the JET data in the pedestal region.

#### 5. ITER model predictions

Preliminary simulations on an ITER grid [9] with a beryllium wall have also been performed including both drifts and a weak ETB, with similar assumptions to those used in JET simulations. The input power was chosen at 84 MW (Fusion power = 410 MW,  $Q = 10$ , 30% core radiation) and the separatrix density at  $1.8 \times 10^{19} \text{ m}^{-3}$ , compared to the expected value  $3.0 \times 10^{19} \text{ m}^{-3}$ . Nonetheless, partial detachment was observed at both inner and outer strike points. The converged solution yields  $T_e^{\text{ped}} \sim 1.7 \text{ keV}$  and  $T_i^{\text{ped}} \sim 2.5 \text{ keV}$  for a  $D_{\perp}^{\min} = 0.25 \text{ m}^2 \text{ s}^{-1}$ . Based on the square root dependence discussed previously, the design value of  $T_i^{\text{ped}} \sim 4 \text{ keV}$  would thus require an ETB with  $D_{\perp}^{\min} = 0.1 \text{ m}^2 \text{ s}^{-1}$ . Such simulations will be performed in a future study.

#### 6. Conclusions

Improved core boundary conditions have been used in the EDGE2D drift model, which allow self-consistent integrated multi-fluid (hydrogen + impurities) modelling with both ETB and drifts. Without drifts, the pedestal pressure, stored energy and energy confinement time increase as  $D_{\perp}^{\min}^{-\frac{1}{2}}$ , ( $D_{\perp}^{\min} = \frac{2}{5} \chi_{\perp}^{\min}$ ) $^{-\frac{1}{2}}$ , a result which is not modified by the inclusion of drifts. The inclusion of drifts has little effect on the power balance for a weak ETB, ( $D_{\perp}^{\min} > 0.5 \text{ m}^2 \text{ s}^{-1}$ ), however for  $D_{\perp}^{\min} < 0.5 \text{ m}^2 \text{ s}^{-1}$  the pedestal (core) carbon content is increased along with the associated radiation by up to 65%, compared with the no drift case. The result is a reduction in  $T_e^{\text{ped}}$  and an increase in  $n_e^{\text{ped}}$  by  $\sim 30\%$ , (such that  $p_e^{\text{ped}}$  is unaffected), and inner target detachment.

EDGE2D is now able to reproduce edge measurements of  $T_e(r)$  in fuelled, high power JET ELMy H-mode discharges, assuming an ETB with  $D_{\perp}^{\min} = 0.4 \text{ m}^2 \text{ s}^{-1}$ . The JET modelling recipe applied to 84 MW ITER discharges, using an ITER grid, predicts that the ITER design value of  $T_i^{\text{ped}}$  of 4 keV would require an ETB with  $D_{\perp}^{\min} = 0.1 \text{ m}^2 \text{ s}^{-1}$ .

#### Acknowledgements

This work was partly funded by the UK Engineering and Physical Sciences Research Council

and by the European Communities under the contract of Association between EURATOM and UKAEA. The view and opinions expressed herein do not necessarily reflect those of the European Commission.

## References

- [1] A. Huber et al., *J. Nucl. Mater.* 337–339 (2005) 241.
- [2] G.S. Kirnev et al., *J. Nucl. Mater.* 337–339 (2005) 271.
- [3] A. Kallenbach et al., *Plasma Phys. Control. Fus.*, 46 (2004) 431.
- [4] R. Zagórski, et al., Drifts in the Edge Plasma, IPP Jülich report, Jul-3829, November 2000.
- [5] H. Bürbaumer et al., *J. Nucl. Mater.* 290–293 (2001) 571.
- [6] B. LaBombard, et al., in: *Fusion Energy 1996* (Proceeding 16th International Conference Montreal, 1996), vol. 1, IAEA, Vienna, 1997, p. 825.
- [7] S.K. Erents, P.C. Stangeby, *Nucl. Fusion* 38 (11) (1998) 1637.
- [8] R.A. Pitts et al., *Rev. Sci. Instrum.* 74 (11) (2003) 4644.
- [9] A.S. Kukushkin et al., *J. Nucl. Mater.* 290–293 (2001) 887.